Study of the Dissociation of $CH_3SCH_3^+$ by Collisional Activation: Evidence of Nonstatistical Behavior†

Y.-J. Chen,‡ P. T. Fenn,‡ Kai-Chung Lau,‡,§ C. Y. Ng,*,‡,§ Chi-Kin Law,|| and Wai-Kee Li*,||

Ames Laboratory, United States Department of Energy, and Department of Chemistry, Iowa State University, Ames, Iowa 50011, and Department of Chemistry, The Chinese University of Hong Kong, Shatin, N.T., Hong Kong

Received: December 11, 2001; In Final Form: April 5, 2002

The collision-induced dissociation (CID) reaction of $CH_3SCH_3^+ + Ar$ was studied in a triple-quadrupole, double-octopole ion−molecule reaction apparatus. The absolute total cross sections for the product ions CH_2SH^+/CH_3S^+, CH_2S^+, CHS^+, and CH_3^+ formed in the CID reaction have been measured in the center-of-mass kinetic energy (E_{cm}) range of 1−19 eV. Using the charge-transfer probing technique, we found that mass-47 product ions are formed in both the CH_2SH^+ and CH_3S^+ structures. The onsets for CH_2SH^+, CH_3S^+, CH_2S^+, CHS^+, and CH_3^+ are consistent with their thermochemical thresholds. The formation of the higher-energy product channel $CH_3S^+ + CH_3$, which involves C−S bond scission, is found to dominate in the E_{cm} range immediately above its onset. The lower-energy channel corresponding to the formation $CH_3SCH_2^+ + H$ is not found. The strong preference observed for the higher-energy channel is in accordance with the conclusions obtained from the CID studies of CH_3SH^+ and $CH_3CH_2SH^+$, providing further evidence that the CID of $CH_3SCH_3^+$ is also nonstatistical. The high yield of $CH_3S^+ + CH_3$ is attributed to the more efficient translational-to-vibrational energy transfer for the C−S stretching modes with lower frequencies than to those for the C−H stretching modes with higher frequencies, along with weak coupling between these vibrational modes with significantly different frequencies of $CH_3SCH_3^+$. In addition, the dissociation pathways deduced are consistent with the results of ab initio calculations at the G3 level.

I. Introduction

Bond-selective dissociation is a process that violates the expectation of a statistical outcome. Most of bond-selective dissociation studies have been focused on the dissociation processes induced by photoexcitation. In our previous collision-induced dissociation (CID) studies[1−3] concerning the measurements of absolute total CID cross sections for collisions of CH_3SH^+ (or $CH_3CH_2SH^+$) + Ar, we have obtained convincing evidence that bond-selective dissociations occur in these CID reactions. In the CID reaction of $CH_3SH^+ + Ar$, the higher-energy product channel $CH_3^+ + SH$, owing to C−S bond rupture, was found to be more favorable than the more stable product channel $CH_2SH^+ + H$ resulting from C−H cleavage. The CID study of $CH_3CH_2SH^+ + Ar$ reveals that the higher-energy channels $CH_3CH_2^+ + SH$ and $CH_3 + CH_2SH^+$ resulting from the C−S and C−C bond scissions, respectively, are the dominant dissociation processes, whereas the lower-energy product channel $CH_3CHSH^+ + H$, corresponding to the methylenic C−H bond breakage in $CH_3CH_2SH^+$, was not found. The selective C−S and C−C bond cleavage processes in the CID reactions of $CH_3SH^+ + Ar$ and $CH_3CH_2SH^+ + Ar$ are attributed to the more efficient translational to C−S vibrational energy transfer and to inefficient energy flow between C−X and X−H (X = C and S) vibrations. These observations suggest that the dissociation of both CH_3SH^+ and $CH_3CH_2SH^+$ via collisional activation is nonstatistical. Interestingly, previous dissociation studies of CH_3SH^+ and $CH_3CH_2SH^+$ using photoionization[2,4−6] and charge-transfer techniques[7] show that the branching ratios of product ions are in quantitative agreement with the predictions of the quasi-equilibrium theory.

In this article, we present the absolute total cross sections for CID products formed in the collisions of $CH_3SCH_3^+ + Ar$. Because $CH_3CH_2SH^+$ and $CH_3SCH_3^+$ are isomers, the comparison of the branching ratios for product channels from the CID of these isomeric ions is expected to shed light on their CID mechanisms. In accordance with CID results described above, $CH_3S^+ + CH_3$ should be a major product channel in the reaction of $CH_3SCH_3^+ + Ar$, as compared to the formation of $CH_2SH^+ + CH_3$ in the CID reaction of $CH_3CH_2SH^+ + Ar$. The successful detection of CH_3S^+ isomer ions formed in the CID reaction of $CH_3SCH_3^+$ using the charge-transfer probing method has been communicated.[8] To rationalize the dissociation pathways for $CH_3SCH_3^+$ and $CH_3CH_2SH^+$, we have also carried out ab initio calculations for this dissociation system at the Gaussian-3 (G3) level of theory.[9]

II. Experimental Section

The experimental arrangement and procedures of the triple-quadrupole, double-octopole (TQDO) photoionization apparatus for cross-section measurements of state-selected ion−molecule reactions have been described in detail previously.[10−12] Briefly, the TQDO apparatus essentially consists of, in sequential order, a vacuum ultraviolet (VUV) photoionization ion source, a reactant quadrupole mass spectrometer (QMS), a lower radio

† Part of the special issue "Jack Beauchamp Festschrift".

* Corresponding authors. E-mail: cyng@chem.ucdavis.edu; wkLi@cuhk.edu.hk.

‡ Iowa State University.

§ Present address: Department of Chemistry, University of California, Davis, California 95616.

|| The Chinese University of Hong Kong.

10.1021/jp014496y CCC: $22.00
Published on Web 06/06/2002

frequency (RF) octopole ion guide reaction gas cell, a middle QMS, an upper RF octopole ion guide reaction gas cell, a product QMS, and a modified[13] Daly-type scintillation ion detector. The TQDO apparatus is partitioned into five chambers, which are separately evacuated by liquid nitrogen or Freon-trapped diffusion pumps.

The photoionization ion source consists of a 0.2-m VUV monochromator (McPherson 234), a hydrogen discharge lamp, and a photoelectric VUV light detector. The ionization energy (IE) for CH_3SCH_3 is known to be 8.6910 ± 0.0002 eV (1426.60 $\pm$ 0.03 Å).[14] In the present experiment, CH_3SCH_3 is introduced into the photoionization source as a free jet formed by supersonic expansion through a nozzle with a diameter of 75 μm at a stagnation pressure of ~120 Torr. By setting the photoionization wavelength at 1420 Å, which has a resolution of 5 Å (full width at half-maximum (fwhm)), the $CH_3SCH_3^+$ reactant ions were formed in their ground vibronic states. The rotational temperature of $CH_3CH_2SH^+$ thus formed is expected to be $\leq$150 K, which is characteristic of the neutral CH_3CH_2SH jet. We note that the finite vibrational excitation of $CH_3SCH_3^+$ due to the thermal population of the low-frequency vibrational modes of $CH_3SCH_3^+$ may not be efficiently relaxed by the mild beam expansion employed in this experiment.

For absolute total cross-section measurements, the reactant $CH_3SCH_3^+$ ions were extracted and guided by the lower QMS (operated in the RF-only mode) and the lower RF octopole ion guide to the middle QMS. The middle QMS, functioning as a mass filter, passed only the desired $CH_3SCH_3^+$ ions to the upper reaction gas cell, where collision-activated dissociation occurred with Ar. The pressure of Ar in the upper reaction gas cell was monitored with an MKS Baratron manometer and was maintained at $(2-3) \times 10^{-4}$ Torr. In this pressure range, the CID product ion intensity was found to have a linear dependence on the Ar gas-cell pressure. The reactant ions and the product ions formed in the upper reaction gas cell were then mass-selected by the product QMS and detected with the Daly-type ion detector.

The reactant ion beam energies were determined by the retarding potential method, using the upper octopole ion guide to retard the reactant $CH_3SCH_3^+$ ions. The retarding potential curve thus obtained was differentiated to yield the most probable laboratory kinetic energy (E_{lab}) of the reactant ions and the fwhm of the kinetic energy distribution. The E_{lab} resolution for $CH_3SCH_3^+$ achieved in this experiment was $\pm$0.2 eV, as measured by the fwhm of the E_{lab} distribution. This value corresponds to a center-of-mass collision-energy (E_{cm}) resolution of $\pm$0.08 eV (fwhm). The collection efficiencies for reactant and product ions were maximized at each E_{cm} by optimizing the voltage settings applied to the ion lenses, the octopole ion guides, and the QMSs. As in previous studies,[1-3] two modes of absolute cross-section measurements were made. One involves the measurement of the relative intensities of a product ion and the reactant ion as a function of E_{lab} at a fixed mass resolution of the product QMS. The other mode of operation involves the accumulation of a mass spectrum in a mass range covering the masses of the reactant and all the product ions. The absolute total cross sections obtained by these modes are in agreement. The latter mode of operation has the advantage of avoiding the mass-drifting problem of the QMS and ensuring that the mass resolution is sufficient to resolve the mass speaks of interest.

To probe the structure of the mass-47 ions formed in the CID reaction of $CH_3SCH_3^+ + Ar$, we used both the lower and upper reaction gas cells. Reactant $CH_3SCH_3^+$ ions prepared by photoionization of CH_3SCH_3 were first selected by the reactant QMS to enter the lower RFOIGGC, where the CID reaction $CH_3SCH_3^+ + Ar$ took place. The Ar gas-cell pressure that was used was 3×10^{-4} Torr. The mass-47 product ions thus formed in the E_{cm} range of 4.5−6.5 eV were selected by the middle QMS and guided into the upper reaction gas cell, in which the structure for the mass-47 ions was probed by the charge-transfer reaction with benzene (C_6H_6) at $E_{cm} \approx 0.2$ eV. Charge-transfer product $C_6H_6^+$ ions, if formed, were detected by the product QMS. The C_6H_6 pressure used in the upper gas cell was 3×10^{-4} Torr. The IEs for CH_3S, CH_2SH, and C_6H_6 are known to be 9.2649 ± 0.0010 eV,[15] 7.536 ± 0.003 eV,[16] and 9.243842 ± 0.000006 eV,[17] respectively (see Table 1). Using these IE values, we calculated[8] charge-transfer reaction 1 for CH_3S^+ to be slightly exothermic, by 0.0211 eV, whereas charge-transfer reaction 2 for CH_2SH^+ is endothermic by more than 1.708 eV. The ΔH_0° values given in reactions 1 and 2 are the corresponding heats of reaction at 0 K.

TABLE 1: Current Recommended Experimental $\Delta_f H_0^\circ$ and IE Values[a]

species	$\Delta_f H_0^\circ$ (kcal/mol)	IE (eV)
CH_3SCH_3	-8.96 ± 0.48[b]	8.69 ± 0.02[b]
CH_2SH	37.7 ± 2.0	7.536 ± 0.003
CH_3S ($^2E_{3/2}$)	31.4 ± 0.5	9.2649 ± 0.0010
CH_3S ($^2E_{1/2}$)		9.2330 ± 0.0010
CH_2S	28.3 ± 2.0	9.376 ± 0.003
CH_4	-17.89[b]	
CH_3	35.6 ± 0.3	9.8380 ± 0.0004
S	66.2 ± 0.04[b]	
H	51.10 ± 0.00014[b]	
$CH_3SCH_3^+$	197.5[c]	
$CH_3SCH_2^+$	197.3[c]	
CH_2SH^+	211.5 ± 2.0	
CH_3S^+	245.0 ± 0.5	
CH_2S^+	244.5 ± 2.0	
HCS^+	243.2 ± 2.9	
H_2S^+	237.2 ± 0.2	
CH_3^+	262.5 ± 0.3[a]	

[a] Reference 2 and references therein. [b] Reference 28. [c] G3 calculation.

$$CH_3S^+ + C_6H_6 \rightarrow CH_3S + C_6H_6^+ \qquad \Delta H_0^\circ = -0.0211 \text{ eV} \tag{1}$$

$$CH_2SH^+ + C_6H_6 \rightarrow CH_2SH + C_6H_6^+ \qquad \Delta H_0^\circ = 1.708 \text{ eV} \tag{2}$$

Becuase near-resonant charge-transfer reactions usually have large cross sections, we should observe the formation of $C_6H_6^+$ if the mass-47 ions have the CH_3S^+ structure, whereas the charge-transfer cross section should be negligibly small if CH_2SH^+ ions are produced.

It is known that CH_2SH^+ ions are produced at the onset by the photoionization of CH_3SH.[18] This conclusion is based on the fact that the thermochemical threshold of $\Delta H_0^\circ = 11.541$ eV for process 3 is very close to the appearance energy (AE) of ~11.55 eV for the mass-47 ion observed in the dissociative photoionization of CH_3SH.

$$CH_3SH + h\nu \rightarrow CH_2SH^+ + H + e^- \qquad \Delta H_0^\circ = 11.541 \text{ eV} \tag{3}$$

The formation of CH_2SH^+ by process 3 has been further confirmed by Fenn et al.[2] using benzene as the charge-transfer probing reactant. The latter experiment can be taken as a validation of the charge-transfer probing technique used here

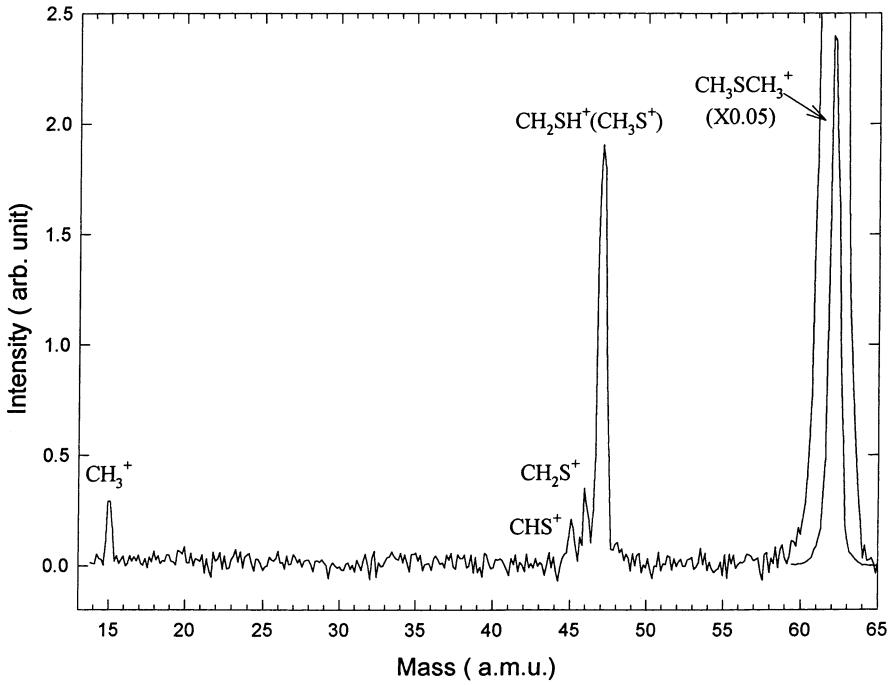

Figure 1. Mass spectrum in the mass range of $m/z = 13-66$ amu for the CID reaction of $CH_3SCH_3^+ + Ar$ obtained at $E_{cm} = 14$ eV. The mass peak for $m/z = 62$ amu has been scaled by a factor of 0.05. Using a higher mass resolution than that used to record this spectrum, we have carefully searched for the mass-61 ion peak at various E_{cm} values and have concluded that $CH_3SCH_2^+$ is not produced in the CID reaction of $CH_3SCH_3^+ +$ Ar within the estimated uncertainty of $\pm 5 \times 10^{-18}$ cm^2 for cross sections measured in the present study. See the text.

for the structural identification of the mass-47 ion (CH_2SH^+ or CH_3S^+) formed in the photoionization and CID reactions.

Data acquisition for the TQDO apparatus was controlled by a Pentium PC.[19] This improvement allows computer control of the QMS and monochromator scans, the voltage settings applied to individual components of the ion optics system, the reactant ion kinetic energy determination, and the background corrections in absolute total cross-section measurements. The procedures outlined above were conducted mostly in an automatic mode.

The dimethyl sulfide and benzene samples were obtained from Aldrich Chemical Company and Fisher Scientific and had purities of 99.5% and 99.9%, respectively. The Ar gas was obtained from Air Products and had a purity of 99.998%.

III. Results and Discussion

A. Absolute Total Cross Section and Identification of CID Product Channels. The mass spectrum of the reactant and product ions formed in the CID reaction of $CH_3SCH_3^+ + Ar$ at $E_{cm} = 14$ eV is displayed in Figure 1, showing the product ion peaks for CH_2SH^+/CH_3S^+, CH_2S^+, CHS^+, and CH_3^+. This mass spectrum indicates that the mass-47 ion with the possible structures of CH_2SH^+ and CH_3S^+ is the overwhelmingly dominant ion among the products. An important finding of this study is that the $CH_2SCH_3^+$ ion (mass 61), which is a fragment ion found in the photoionization of CH_3SCH_3 (see section III.B.), is not observed in the CID reaction of $CH_3SCH_3^+ + Ar$ within the estimated uncertainty of $\pm 5 \times 10^{-18}$ cm^2 for absolute cross sections measured in this CID study. This conclusion was reached by using a higher mass resolution than that used for recording the mass spectrum shown in Figure 1. We have also carefully examined the reactant mass peak with and without Ar gas in the upper reaction gas cell at various E_{lab} values. In both experiments, we found no evidence of the mass-61 peak (or the formation of $CH_2SCH_3^+$).

The absolute total cross sections for CH_2SH^+/CH_3S^+, CH_2S^+, CHS^+, and CH_3^+ that were measured as a function of E_{cm} over

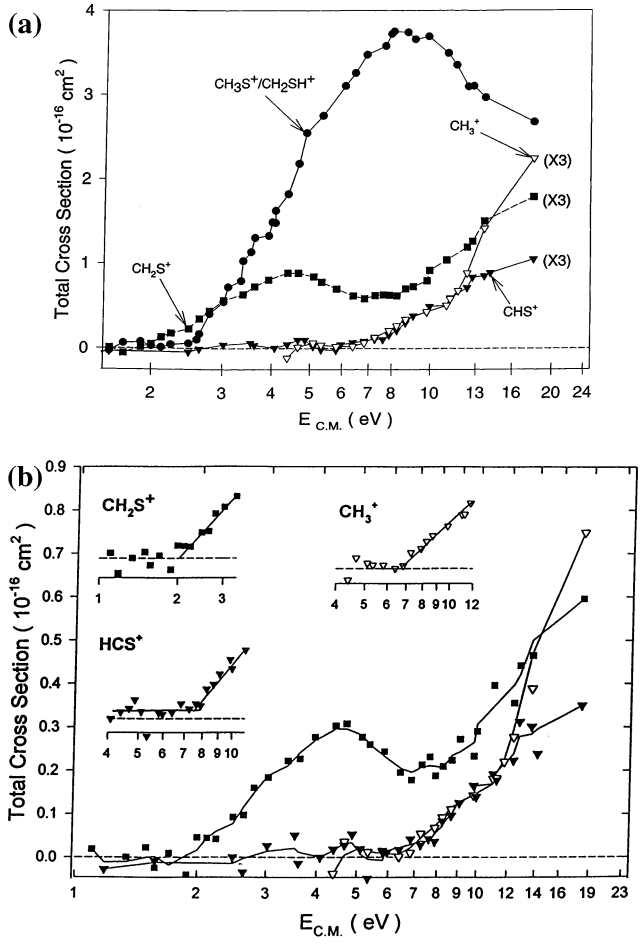

Figure 2. Absolute total cross-section curves for (a) CH_3S^+ (●), CH_2S^+ (■), CHS^+ (▼) and CH_3^+ (▽) (the curves for CH_2S^+, CHS^+, and CH_3^+ have been scaled by a factor of 3) and (b) CH_2S^+ (■), CHS^+ (▼), and CH_3^+ (▽) formed in the CID reaction of $CH_3SCH_3^+ + Ar$ at $E_{cm} = 1.2-19$ eV.

the range 1.2−19 eV are shown in Figure 2a. The cross-section curve of the major product ion CH_2SH^+/CH_3S^+ is sensitive to E_{cm}, exhibiting a maximum of 3.8 Å^2 at E_{cm}= 8−10 eV. The kinetic energy dependence of this cross-section curve is quite different from the mass-47 ion formed in the CID reaction of isomeric $CH_3CH_2SH^+ + Ar$, where the cross-section curve is nearly constant from $E_{cm} \approx 3.5$ eV.[3]

The cross section of CH_2S^+ exhibits a small maximum at $E_{cm} \approx 4.8$ eV and shows a more steeply sloping increase from $E_{cm} \approx 8$ eV. The other two minor product ions, CHS^+ and CH_3^+, have very gradual increases in their cross sections as E_{cm} is increased, which is typical for product ions from secondary dissociation processes. A magnified view of the cross-section curves for these minor product ions is depicted in Figure 2b. It is interesting that the profiles of the cross sections for CHS^+ and CH_3^+ are strikingly similar in their E_{cm} ranges from their onsets to ~13 eV.

Using the known thermochemical data listed in Table 1, the corresponding ΔH_0° values for the possible CID product channels are given below:

$$CH_3SCH_3^+ + Ar \rightarrow CH_3SCH_2^+ + H + Ar \qquad \Delta H_0^\circ = 2.21 \text{ eV} \quad (4)$$

$$\rightarrow CH_2SH^+ + CH_3 + Ar \qquad \Delta H_0^\circ = 2.15 \text{ eV} \quad (5a)$$

$$\rightarrow CH_3S^+ + CH_3 + Ar \qquad \Delta H_0^\circ = 3.60 \text{ eV} \quad (5b)$$

$$\rightarrow CH_2S^+ + CH_4 + Ar \qquad \Delta H_0^\circ = 1.26 \text{ eV} \quad (6a)$$

$$\rightarrow CH_2S^+ + H + CH_3 + Ar \qquad \Delta H_0^\circ = 5.80 \text{ eV} \quad (6b)$$

$$\rightarrow CHS^+ + H + CH_4 + Ar \qquad \Delta H_0^\circ = 3.42 \text{ eV} \quad (7a)$$

$$\rightarrow CHS^+ + H_2 + CH_3 + Ar \qquad \Delta H_0^\circ = 3.53 \text{ eV} \quad (7b)$$

$$\rightarrow CHS^+ + 2H + CH_3 + Ar \qquad \Delta H_0^\circ = 7.96 \text{ eV} \quad (7c)$$

$$\rightarrow CH_3^+ + CH_3S + Ar \qquad \Delta H_0^\circ = 4.18 \text{ eV} \quad (8a)$$

$$\rightarrow CH_3^+ + CH_2SH + Ar \qquad \Delta H_0^\circ = 4.44 \text{ eV} \quad (8b)$$

$$\rightarrow CH_3^+ + CH_3 + S + Ar \qquad \Delta H_0^\circ = 7.23 \text{ eV} \quad (8c)$$

All of the atomic and molecular species in the above reactions are assumed to be in their ground states. To identify the corresponding dissociation channels responsible for the product ions, the experimental appearance energies (AEs) for CH_2SH^+, CH_2S^+, CHS^+, and CH_3^+ are summarized in Table 2. We note that the experimental AE values of these product ions represent upper limits of corresponding dissociation energies, and the uncertainties assigned to the AEs are determined by the precision of the measurements.

TABLE 2: Appearance Energies (AEs) and E_{ex} Onset Values

product ions	CID[a] AE (eV)	photoionization[a,b] E_{ex} onset (eV)
$CH_3SCH_2^+$		2.24 ± 0.06[a]
		(1.284 ± 0.02)[c]
CH_2SH^+/CH_3S^+	2.6 ± 0.2	2.20 ± 0.06[a]
		(2.03 ± 0.018)[c]
CH_2S^+	2.0 ± 0.2	1.90 ± 0.06[a]
		(1.814 ± 0.018)[c]
CHS^+	7.6−8.2	
CH_3^+	6.8−7.3	

[a] This work. Appearance energy was determined in the CID study of $CH_3SCH_3^+(1^2A'') + Ar$. The uncertainties represent the precision of the measurements. [b] E_{ex} onset = AE(PI) − IE(CH_3SCH_3), where AE(PI) is the AE determined in the photoionization of CH_3SCH_3. [c] Reference 25.

The AE value observed for the mass-47 ion is 2.6 ± 0.2 eV, which is slightly higher than the thermochemical threshold of $\Delta H_0^\circ = 2.15$ eV of reaction 5a. This observation indicates that CH_2SH^+ is formed near the CID AE for the mass-47 ion. The protonated thioformaldehyde[16] (CH_2SH^+) and thiomethoxy[2] (CH_3S^+) ions are both stable isomers, and the latter is 1.45 eV higher in energy than the former. On the basis of the charge-transfer probing experiment, previous CID studies[20,21] on CH_3SH^+ and $CH_3CH_2SH^+$ show that the mass-47 ion formed near the AE has the structure of protonated thioformaldehyde, CH_2SH^+. Ab initio studies[21,22] suggest that the CH_2SH^+ ion from collision-activated $CH_3SCH_3^+$ may be produced via a two-step rearrangement−dissociation mechanism. It involves H rearrangement of $CH_3SCH_3^+$ via a tight transition complex to form $CH_2SHCH_3^+$, which subsequently dissociates to form CH_2SH^+ by breaking the C−S bond of $CH_2SHCH_3^+$. At higher internal excitation of $CH_3SCH_3^+$, we expect that direct cleavage of the $CH_3S^+-CH_3$ bond to form CH_3S^+ will compete with the dissociation of the tight transition complex to form CH_2SH^+.

To identify the isomeric structures (i.e., CH_2SH^+ and CH_3S^+) of the mass-47 ions formed by the CID reaction of $CH_3SCH_3^+ + Ar$, we performed a charge-transfer probing experiment using benzene as described above. As previously indicated, charge-transfer product $C_6H_6^+$ should be observed if the mass-47 product ion has the CH_3S^+ structure, whereas the intensity for charge-transfer product $C_6H_6^+$ will be negligibly small if CH_2SH^+ is formed, provided that the E_{cm} value for the charge-transfer probing reaction is kept below the endothermicity of 1.708 eV for reaction 2. The total cross-section curve for the $m/z = 47$ ion formed in the CID reaction of $CH_3SCH_3^+ + Ar$ is shown again[8] in Figure 3a to compare with the cross-section curve for $C_6H_6^+$ resulting from the probing charge-transfer reactions between C_6H_6 and the mass-47 ions formed in the CID reaction of $CH_3SCH_3^+ + Ar$ in the E_{cm} range of 2−7 eV. As shown in Figure 3b, the cross-section curve of $C_6H_6^+$ is found to have a sharp onset at $E_{cm} = 3.6 \pm 0.2$ eV, which is indicative of the formation of CH_3S^+ at $E_{cm} \geq 3.6$ eV. This onset E_{cm} value is in excellent agreement with the thermochemical threshold of $\Delta H_0^\circ = 3.60$ eV for reaction 5b. This observation indicates that pure CH_2SH^+ is produced in the E_{cm} range of 2.6−3.6 eV, whereas CH_3S^+ is produced in abundance along with CH_2SH^+ in the CID reaction of $CH_3SCH_3^+ + Ar$ at $E_{cm} \geq 3.6$ eV. We have also included in Figure 3a the total cross-section curve for the $m/z = 47$ ion formed in the CID reaction of $CH_3CH_2SH^+ + Ar$.[3] As mentioned above, the $m/z = 47$ ions formed in the latter reaction were found to have the CH_2SH^+ structure on the basis of the previous charge-transfer

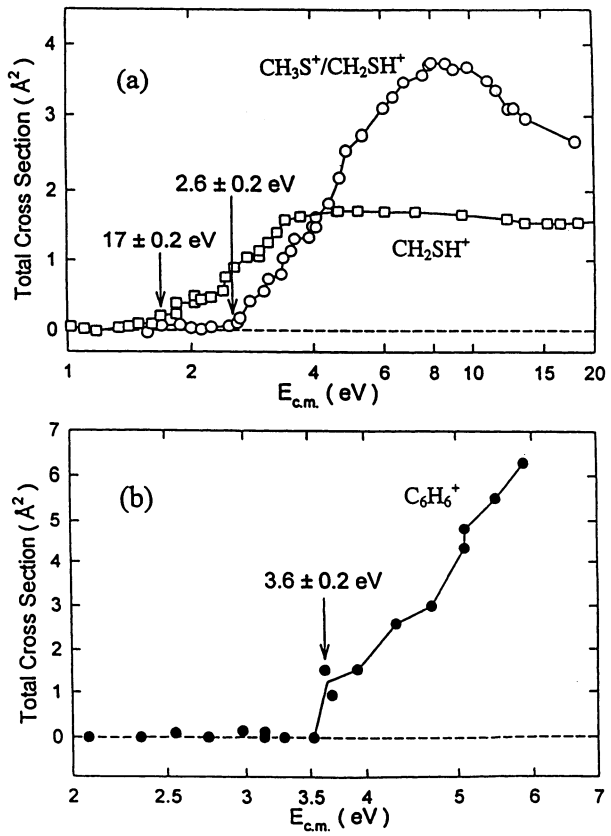

Figure 3. (a) Absolute total cross-section curves (○) for the mass-47 ion formed in the CID reaction of $CH_3SCH_3^+ + Ar$ (O) and $CH_3CH_2SH^+ + Ar$ (□) at $E_{cm} = 1-20$ eV. (b) Absolute cross section for $C_6H_6^+$ observed in the charge-transfer reaction of C_6H_6 with the mass-47 ion at a fixed E_{cm} of 0.2 eV. The mass-47 ions are formed in the CID reaction of $CH_3SCH_3^+ + Ar$ at $E_{cm} = 2-7$ eV. We note that the E_{cm} onset at 3.6 ± 0.2 eV is in agreement with the threshold of 3.60 eV for reaction 5b.

probing experiment. The total cross-section curve for the $m/z = 47$ ion from $CH_3CH_2SH^+ + Ar$ rises from the threshold for the formation of CH_2SH^+ at 1.7 eV and becomes essential constant at ~1.6 Å^2 in the E_{cm} range of 3.5−20 eV. Comparing the cross-section curves for $C_6H_6^+$ in Figure 3b with those for the mass-47 ions from $CH_3SCH_3^+ + Ar$ and $CH_3CH_2SH^+ + Ar$ in Figure 3a, we may conclude that the further rise in the CID cross section for the mass-47 ion from $CH_3SCH_3^+ + Ar$ at $E_{cm} \geq 3.6$ eV is most likely caused by the opening of the $CH_3S^+ + CH_3$ product channel (reaction 5b).

The experimental AE for the formation of CH_2S^+ is found to be 2.0 ± 0.2 eV. Although this value is significantly higher than the thermochemical threshold of $\Delta H_0^\circ = 1.26$ eV for reaction 6a, the observed AE should correspond to the value for the formation of $CH_2S^+ + CH_4$. The difference of 0.74 eV between the experimental AE and the thermochemical threshold can be ascribed to an activation barrier for the H migration from one methyl group to the other. The fast rise after the plateau at ~7.5 eV suggests the opening of a new product channel. By linearly extrapolating the rising cross-section curve to the plateau region, we estimate that the onset for this new product channel may be at $E_{cm} = 7.3 \pm 0.5$ eV. Taking into account the large uncertainty due to linear extrapolation and the internal energy distribution of the intermediate state, we attribute the rise of the cross section at 7.3 eV to the further dissociation of excited product ions CH_2SH^+ and CH_3S^+ (product channels 5a and 5b) to form $CH_2S^+ + H + CH_3$ (product channel 6b). The formation of other isomers, such as *cis*- and *trans*-$HCSH^+$, is possible at higher collision energies. These latter isomers are estimated to be 1.1 eV higher in energy than CH_2S^+.[3]

The experimental AE(HCS^+) determined in the range of 7.6−8.2 eV is significantly higher than the thermochemical threshold of $\Delta H_0^\circ = 3.42$ and 3.53 eV for reaction 7a or 7b, respectively, but is in reasonable agreement with the value $\Delta H_0^\circ = 8.01$ eV for reaction 7c. Thus, we may conclude that the formation of the major fraction of HCS^+ is likely accompanied by the production of $2H + CH_3$. However, HCS^+ ions may still be contributed by product channels 7a and 7b, accompanied by the formation of $H_2 + CH_3$ or $H + CH_4$, respectively. Product channel 7a may result from H_2 elimination from internally excited CH_2SH^+/CH_3S^+ formed in reactions 5a and 5b, whereas product channel 7b may be formed by the further dissociation of excited CH_2S^+ formed in reaction 6a.

The AE for the formation of CH_3^+ was determined to be in the range of 6.8−7.3 eV. Because the value is lower than the thermochemical threshold of $\Delta H_0^\circ = 7.23$ eV for reaction 8c, we can exclude the possibility of secondary dissociation of CH_3S^+ to form $CH_3^+ + S$ in the threshold region. Although the AE of 6.8−7.3 eV is significantly higher than the value corresponding to thermochemical thresholds of ΔH_0° for reactions 8a and 8b, 4.16 and 4.44 eV, respectively, we may still attribute the formation of CH_3^+ near the AE to direct scission of the C−S bond from reactant ions. The very gradual rise at the threshold and the small cross section are to be expected for the less-favored formation of CH_3^+ compared to that of CH_2SH^+ (CH_3S^+). Because IE(CH_3) = 9.8380 ± 0.0004 eV[23] is significantly higher than IE(CH_2SH) = 7.536 ± 0.003 eV[16] (IE(CH_3S) = 9.2649 ± 0.0010 eV), the charge is thus much less likely to reside on CH_3 during the dissociation process.

B. Comparison of Product Ions and Their Branching Ratios Observed in CID and Photoionization. The relative abundances (in percentages) of the product ions, CH_2SH^+/CH_3S^+, CH_2S^+, CHS^+, and CH_3^+, in the CID reaction of $CH_3SCH_3^+$ are shown in Figure 4a. The sum of the abundances for all of the product ions is normalized to 100%. The CH_2S^+ ion, the most stable product channel accompanied by the formation of CH_4, tends to dominate at low energy. The formation of CH_2SH^+/CH_3S^+ dominates in the whole E_{cm} range beginning from its AE at 2.6 eV. The abundances for other minor product ions are negligible below $E_{cm} \approx 7$ eV and start to increase gradually beginning from their corresponding onsets, about where the CH_2SH^+/CH_3S^+ decreases monotonically toward high energy. This observation can be taken as evidence that CH_2SH^+/CH_3S^+ ions are precursor ions for the other minor ions.

To examine possible differences between the dissociation mechanisms via collisional activation and photoionization, we have also measured the photoionization efficiency (PIE) curves at photon energy of up to 13 eV. Because the PIE curves for $CH_3SCH_3^+$, $CH_3SCH_2^+$, CH_2SH^+/CH_3S^+, and CH_2S^+ are in good agreement with those reported previously,[24,25] the spectra are not presented in this paper. The observed AE values for the formation of $CH_3SCH_2^+$, CH_2SH^+/CH_3S^+, and CH_2S^+ in photoionization are listed in Table 2 to compare with those values determined in CID. To compare the product abundances observed in photoionization with those in CID, the photon energies ($h\nu$) in PIE measurements are converted into maximum excitation energies (E_{ex}) of $CH_3SCH_3^+$ by the relation $E_{ex} = h\nu - IE(CH_3SCH_3)$. That is, E_{ex} in the photoionization experiment is equivalent to E_{cm} in the CID experiment, which is used to determine the maximum excitation energy for $CH_3SCH_3^+$ via collisional activation.

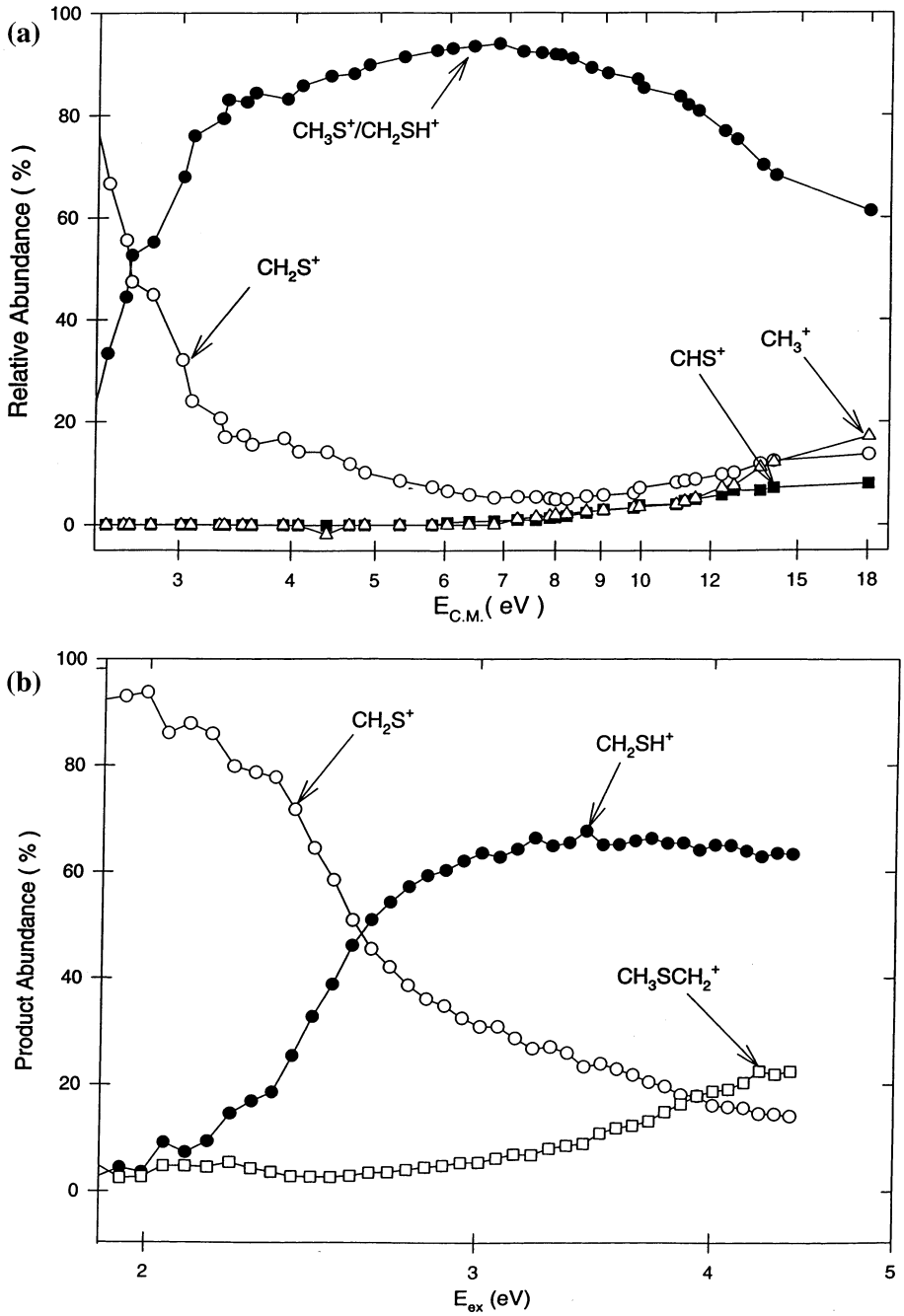

Figure 4. Relative percentage abundances of the product ions (a) CH_2SH^+/CH_3S^+ (●), CH_2S^+ (○), CHS^+ (■), and CH_3^+ (△) observed in the CID reaction of $CH_3SCH_3^+ + Ar$ in the E_{cm} range of 2−18 eV and (b) $CH_3SCH_2^+$ (□), CH_2SH^+ (●), and CH_2S^+ (○) observed in the photoionization of CH_3SCH_3 in the E_{ex} range of 1.9−4.5 eV, where $E_{ex} = h\nu - IE(CH_3SCH_3)$.

The most significant difference between the CID and photoionization results is that the formation of $CH_3SCH_2^+$ observed in photoionization is not observed in the CID experiment. The E_{ex} onset of 2.24 ± 0.06 eV observed for $CH_3SCH_2^+$ is in agreement with the predicted value of $\Delta H_0^\circ = 2.21$ eV for reaction 4. After comparing the E_{ex} onset value of 2.20 ± 0.06 eV for the mass-47 ion with the thermochemical threshold of $\Delta H_0^\circ = 2.15$ eV for reaction 5a, we conclude that CH_2SH^+ is formed near the photoionization threshold. To examine the existence of its isomer CH_3S^+ at higher energy, we use the charge-transfer reaction with C_6H_6 to probe the structure of the mass-47 ions. The fact that no charge-transfer product $C_6H_6^+$ ions were observed indicates that the mass-47 ions formed in the photoionization of CH_3SCH_3 have the CH_2SH^+ structure. It is interesting that the photoionization of CH_3CH_2SH, an isomer of CH_3SCH_3, also produces the same isomeric structure for the mass-47 ions. Although the E_{ex} onset of 1.90 ± 0.06 eV for CH_2S^+ observed in the photoionization of CH_3SCH_3 is slightly higher than the thermochemical threshold of $\Delta H_0^\circ = 1.26$ eV of reaction 6a, we may still conclude that the $CH_2S^+ + CH_4$ channel is formed near its AE in photoionization.

Figure 4b shows the relative abundances (in percentages) of the product fragment ions, $CH_3SCH_2^+$, CH_2SH^+, and CH_2S^+, observed in the photoionization of CH_3SCH_3. The sum of the abundances for all of the products except $CH_3SCH_3^+$ is normalized to 100% for the purpose of comparison with that in the current CID experiment. The endothermicity for the formation of $CH_2S^+ + CH_4$ is lower than that of $CH_3SCH_2^+ + H$ and $CH_2SH^+ + CH_3$. The high yield observed at $E_{cm} < 2.3$ eV for CH_2S^+ is consistent with the prediction because the

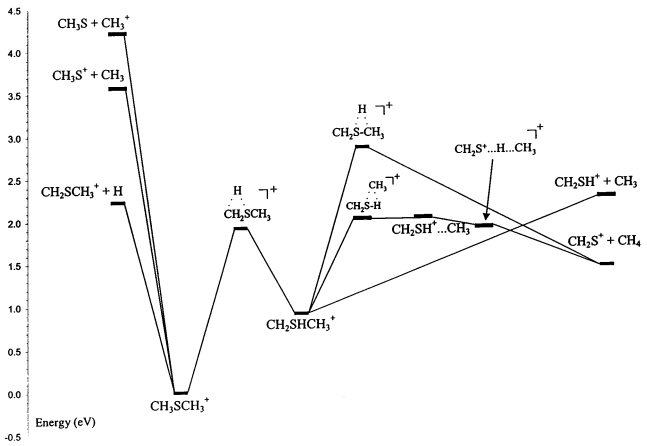

Figure 5. Potential energy profile for the rearrangement and dissociation reactions of $CH_3SCH_3^+$. The energies shown are calculated at the G3 level of theory. The geometrical structures for the species involved are not shown.

formation of $CH_2S^+ + CH_4$ is the only energetically allowed dissociation channel in the low E_{cm} range. As the excitation energy increases to beyond ~2.6 eV, the abundance of CH_2SH^+ becomes greater than that of CH_2S^+.

C. Ab Initio Gaussian-3 Study of the Dissociation Pathway of $CH_3SCH_3^+$. To rationalize the dissociation pathways observed in this study, we have calculated the stabilities and structures of possible transition structures (TSs) and product channels involving the dissociation reactions of $CH_3SCH_3^+$ using G3 theoretical procedures. The calculated potential energies for possible rearrangement and dissociation pathways leading to the formation of $CH_3SCH_2^+$, CH_2SH^+/CH_3S^+, CH_2S^+, CHS^+, and CH_3^+ are depicted in Figure 5.

The dissociation reactions of $CH_3SCH_3^+$ to form $CH_3SCH_2^+ + H$, $CHS^+ + CH_3 + 2H$, and $CH_3^+ + CH_3S$, which involve the cleavage of either a C−H or a C−S bond or both, are predicted to have no potential barrier. These theoretical predictions are consistent with the experimental observation that the observed AE and E_{ex} values for these product channels agree with the corresponding thermochemical thresholds. However, the formation of CH_2SH^+ and CH_2S^+ from $CH_3SCH_3^+$ is believed to involve TSs. The isomer ion $CH_2SHCH_3^+$ is predicted to be a stable species, which can be formed by a 1,2 H shift from $CH_3SCH_3^+$. This isomeric ion is calculated to be 0.91 eV less stable than $CH_3SCH_3^+$. A TS for the 1,2 H shift links $CH_3SCH_3^+$ to $CH_2SHCH_3^+$, and the barrier is 1.91 eV. Hence, at excitation energies greater than 1.91 eV, these two isomeric structures can interconvert and contribute to the dissociation product ions. The CID threshold of 2.6 ± 0.2 eV for the formation of $CH_2SH^+ + CH_3$ is higher than the transition barrier of 1.91 eV, so the rearrangement of the parent ion $CH_3SCH_3^+$ via a 1,2 H shift is expected to proceed prior to dissociation. The direct cleavage of the $H_2C(H)S^+-CH_3$ bond occurs without a barrier, forming CH_2SH^+ and CH_3. As the excitation energy is increased above the AE for CH_3S^+, the dissociation of $CH_3SCH_3^+$ to form $CH_3S^+ + CH_3$, which involves the direct breakage of the $CH_3S^+-CH_3$ bond, becomes a plausible alternative.

Both the values of AE = 2.0 ± 0.2 eV and E_{ex} = 1.9 ± 0.06 eV for the formation of CH_2S^+ ions are higher than the thermochemical threshold of $\Delta H_0^\circ = 1.26$ eV for reaction 6a, indicating that a potential energy barrier of ~0.75 eV may exist above the energy of $CH_2S^+ + CH_4$. Bearing this expectation in mind, we have located a TS for this H shift between the S and methyl C atoms, and this TS has a G3 transition barrier of 1.43 eV above $CH_2S^+ + CH_4$ (leading to an overall effective barrier of 2.84 eV). This calculated barrier is significantly higher than the experimental value of 2.0 ± 0.2 eV, which suggests that this H-shift TS may not be responsible for the dissociation and rearrangement of $CH_2SHCH_3^+$ to $CH_2S^+ + CH_4$. Nevertheless, we have located another TS for the methyl shift across the S−H bond. This TS leads to the formation of the $CH_2SH^+\cdots CH_3$ complex and is followed by H abstraction from the methyl group to yield $CH_2SH^+ + CH_4$. The respective potential energy barriers for the methyl shift and the H abstraction are calculated to be 0.60 and 0.48 eV, respectively, above $CH_2SH^+ + CH_4$. Thus, the dissociation from $CH_3SCH_3^+$ to $CH_2S^+ + CH_4$ is governed by the potential energy barrier of the methyl shift between $CH_2SHCH_3^+$ and $CH_2SH^+\cdots CH_3$. The calculated overall potential barrier of 2.01 eV is consistent with our experimental finding of 2.0 ± 0.2 eV.

The formation of HCS^+ can be accomplished by the further elimination of H from products $CH_2SH^+ + CH_3$ and $CH_2S^+ + CH_4$. These stepwise pathways (not shown in Figure 5), which result in the formation of $CHS^+ + CH_3 + 2H$, are predicted to proceed without a potential barrier.

D. Dissociation Mechanisms for Collision-Activated $CH^3SCH_3^+$. In the E_{cm} range of this CID experiment, the collisions are the most efficient to promote translational−vibrational and translational−rotational energy exchanges. On the other hand, the electronic excitation by low-energy collisions is known to be highly inefficient. In the previous CID investigation of the $CH_3SH^+ + Ar$ system, the observation that the formation of $CH_3^+ + SH$ dominates the more stable product channel $CH_2SH^+ + H$ is contrary to the QET prediction. The highest vibrational frequencies of CH_3SH^+ correspond to the C−H and SH stretching modes with harmonic frequencies of 2556−3035 cm^{-1}, whereas the C−S stretching frequency of 687 cm^{-1} is the second lowest. Fenn et al.[2] argue that the internal vibrational energy of $CH_3CH_2SH^+$ resulting from collisions with Ar is predominantly deposited in the C−S stretching mode instead of the C−H or S−H stretching modes of CH_3SH^+. Owing to the large difference in vibrational frequencies between the C−S and C−H (or S−H) stretching modes of CH_3SH^+, the C−S and C−H (or S−H) stretching modes are only weakly coupled (i.e., the energy flow between the C−S and C−H (or S−H) vibrational modes of CH_3SH^+ is inefficient). As a consequence, the product CH_3^+ ion, which results from the C−S bond cleavage, is favored over the product CH_2SH^+ ions resulting from the cleavage of the $H-CH_2SH^+$ bond.

This current CID study of $CH_3SCH_3^+ + Ar$, together with the previous study of $CH_3CH_2SH^+ + Ar$, can be considered to be a further test for the proposed dissociation scheme on the CID of $CH_3SH^+ + Ar$. On the basis of recent experimental and ab initio calculations,[26] the stretching frequencies associated with the C−H, S−H, and C−S bonds are similar to those of CH_3SH^+.[27,28] The C−C stretching mode of $CH_3CH_2SH^+$ has a frequency of 1000 cm^{-1},[2,26] which is higher than the C−S stretching frequency of 617 cm^{-1} but significantly lower than the C−H (S−H) stretching frequencies of ~3000 cm^{-1}. In addition to the more efficient excitation of the C−S and C−C stretching modes via collisional activation, the coupling between the C−S and C−C modes of $CH_3CH_2SH^+$ should also be more efficient. Owing to the large frequency difference between the C−S (C−C) and C−H (S−H) stretching modes, the coupling or energy flow between the C−S (C−C) and C−H (S−H) stretching modes may remain small on the time scale of the dissociation process. Consequently, product channels arising from the cleavage of the C−S and C−C bonds may dominate

in the collisional-activated dissociation of $CH_3CH_2SH^+$. This expectation is confirmed by the dominant abundance of the $CH_3CH_2^+$ and CH_2SH^+ ions observed in the CID experiment. The failure to observe CH_3CHSH^+ from H elimination, which is the most stable product channel, is attributed to the high vibrational frequency of the C−H mode and the inefficient energy flow between the C−H and C−S (C−C) stretching modes. These results suggest that the collisional-activated dissociation reaction of $CH_3CH_2SH^+$ is not consistent with the QET prediction. The vibrational frequencies of C−S and C−H bonds in $CH_3SCH_3^+$ are similar to those in $CH_3CH_2SH^+$. The C−S stretching mode has a frequency of 660 cm^{-1}, which is significantly lower than the C−H (S−H) stretching frequency of 3000 cm^{-1}. Thus, the internal energy resulting from collisional activation is predominantly deposited in the C−S stretching mode rather than the C−H (S−H) stretching modes. In addition, the coupling between the C−S and C−H (S−H) stretching modes will be inefficient because of the large differences in their vibrational frequencies. Hence, the product ions CH_2SH^+/CH_3S^+ resulting from the rupture of the C−S bond are favored over those from the cleavage of C−H or S−H bonds of $CH_3SCH_3^+$. The observation that the formation of $CH_2S^+ + CH_4$ and CH_2SH^+/CH_3S^+ dominates in low and high E_{cm} ranges, respectively, is consistent with expectations. The failure to observe $CH_3SCH_2^+$, which was produced in photoionization, further confirms the conclusion that the CID reactions of those species are nonstatistical in nature.

We note that the requirement for the conservation of orbital angular momentum in bimolecular collisions might partially inhibit the H-loss channel, such as the formation of $CH_3SCH_2^+ + H$ from $CH_3SCH_3^+ + Ar$. However, this effect alone cannot account for the fact that we did not observe $CH_3SCH_2^+$ in the full E_{cm} range of interest in the present study.

IV. Conclusions

In the present work, the CID reaction of $CH_3SCH_3^+ + Ar$ has been investigated using a TQDO photoionization apparatus. The absolute total cross sections for the product ions CH_2SH^+/CH_3S^+, CH_2S^+, CHS^+, and CH_3^+ formed in the CID reaction have been measured in the E_{cm} range of 1−19 eV. In addition, the AEs of these product ions, as well as that of $CH_3SCH_2^+$, have also been measured using CID and photoionization methods. By means of the charge-transfer probing technique, we found that the mass-47 product ions formed in the CID reaction of $CH_3SCH_3^+ + Ar$ consist of both CH_2SH^+ and CH_3S^+ isomers. The onsets for CID product ions CH_2SH^+, CH_2S^+, CHS^+, and CH_3^+ are consistent with their thermochemical thresholds. Also, the higher-energy channel $CH_3S^+ + CH_3$, which involves C−S bond scission, is found to dominate in the E_{cm} range immediately above its onset. However, the lower-energy channel, corresponding to the formation $CH_3SCH_2^+ + H$, is not observed from CH_3SCH_3 via collisional activation. Such a strong preference for the higher-energy channel is in agreement with the conclusion obtained in previous CID studies of CH_3SH^+ and $CH_3CH_2SH^+$, indicating that the CID of $CH_3SCH_3^+$ is also nonstatistical. The high yields of products $CH_3S^+ + CH_3$ are attributed to the more efficient translational-to-vibrational energy transfer for the low-energy C−S stretching modes than for the high-energy C−H stretching modes and to the weak coupling between these vibrational modes with low and high frequencies of $CH_3SCH_3^+$. We have also rationalized the dissociation pathways of $CH_3SCH_3^+$ leading to product channels observed in this work by using G3 calculations.

Acknowledgment. This work was supported by the Director, Office of Energy Research, Office of Basic Energy Sciences, Chemical Science Division of the U. S. Department of Energy under contract no. W-7405-Eng-82 for the Ames Laboratory. Ames Laboratory is operated for the U.S. Department of Energy by Iowa State University. C.Y.N. also acknowledges support by the NSF ATM 0001644 and AFOSR grant no. F49620-99-1-0234. C.K.L. and W.K.L. thank the Computer Services Centre of the Chinese University of Hong Kong for the allocation of computer time on the SGI Origin 2000 High Performance Server. The work described in this paper was partially supported by a grant from the Research Grants Council of the Hong Kong Special Administrative Region (project no. CUHK4275/00P).

References and Notes

(1) Chen, Y.-J.; Fenn, P. T.; Stimson, S.; Ng, C. Y. *J. Chem. Phys.* **1997**, *106*, 8274.
(2) Fenn, P. T.; Chen, Y.-J.; Stimson, S.; Ng, C. Y. *J. Phys. Chem.* **1997**, *101*, 6513.
(3) Chen, Y.-J.; Stimon, S.; Fenn, P. T.; Ng, C. Y.; Li, W.-K.; Ma, N. L. *J. Chem. Phys.* **1998**, *108*, 8020.
(4) Akopyan, M. E.; Serhiev, Y. L.; Vilesov, F. I. *Klim. Vys. Energy* **1970**, *4*, 305.
(5) Kutina, R. E.; Edwards, A. K.; Berkowitz, J. *J. Chem. Phys.* **1982**, *77*, 5508.
(6) Nourbakhsh, S.; Norwood, K.; Yin, H.-M.; Liao, C.-L.; Ng, C. Y. *J. Chem. Phys.* **1991**, *95*, 945.
(7) Jonsson B.-Ö.; Bind, J. *J. Chem. Soc., Faraday Trans. 2* **1974**, *70*, 1399.
(8) Chen, Y.-J.; Fenn, P. T.; Ng, C. Y. *Chem. Phys. Lett.* **2001**, *336*, 105.
(9) Curtiss, L. A.; Raghavachari, K.; Redfern, P. C.; Rassolov, V.; Pople, J. A. *J. Chem. Phys.* **1998**, *109*, 7764.
(10) Shao, J.-D.; Ng, C. Y. *J. Chem. Phys.* **1986**, *84*, 4317. Shao, J.-D.; Li, Y.-G.; Flesch, G. D.; Ng, C. Y. *Chem. Phys.* **1987**, *86*, 170. Flesch G. D.; Ng, C. Y. *Chem. Phys.* **1991**, *94*, 2372. Flesch, G. D.; Nourbakhsh, S.; Ng, C. Y. *Chem. Phys.* **1990**, *92*, 3490. Flesch G. D.; Ng, C. Y. *Chem. Phys.* **1990**, *92*, 3235.
(11) Ng, C. Y. In *State-Selected and State-to-State Ion−Molecule Reaction Dynamics: I. Experiment*; Ng, C. Y., Baer, M., Eds.; Wiley: New York, 1992. Ng, C. Y. *Adv. Chem. Phys.* **1992**, *82*, 401.
(12) Li, X.; Huang, Y.-L.; Flesch, G. D.; Ng, C. Y. *Rev. Sci. Instrum.* **1994**, *65*, 3724. Li, X.; Huang, Y.-L.; Flesch, G. D.; Ng, C. Y. *Rev. Sci. Instrum.* **1995**, *66*, 2871.
(13) Gibbs, H. M.; Cummins, E. D. *Rev. Sci. Instrum.* **1966**, *37*, 1385.
(14) Cheung, Y. S.; Ng, C. Y. *Int. J. Mass Spectrom. Ion Processes* **1999**, *533*, 185.
(15) Hsu, C.-W.; Ng, C. Y. *J. Chem. Phys.* **1994**, *101*, 5596.
(16) Rusic, B.; Berkowitz, J. *J. Chem. Phys.* **1992**, *97*, 1818.
(17) Neuhauser, R. G.; Siglow, K.; Neusser, H. J. *J. Chem. Phys.* **1997**, *106*, 896.
(18) Kutina, R. E.; Edwards, A. K.; Berkowitz, J. *J. Chem. Phys.* **1974**, *77*, 5508.
(19) Li, X. Ph.D. Thesis, Iowa State University, Ames, IA, 1996.
(20) Dill, D.; McLafferty, F. W. *J. Am. Chem. Soc.* **1979**, *100*, 2907.
(21) Dill, D.; McLafferty, F. W. *J. Am. Chem. Soc.* **1979**, *101*, 6526.
(22) Nobes, R. H.; Bouma, W. J.; Radom, L. *J. Am. Chem. Soc.* **1984**, *106*, 2774.
(23) Bush, J. A.; Chen, P.; Weimann, R. T.; White, M. G. *J. Chem. Phys.* **1993**, *98*, 3557.
(24) Ermolenko, A. I.; Sergeev, Y. L.; Vilesov, F. I. *High Energy Chem.* **1983**, *17*, 19.
(25) Nourbakhsh, S.; Norwood, K.; Yin, H.-M.; Liao, C. L.; Ng, C. Y. *J. Chem. Phys.* **1991**, *95*, 5014.
(26) Cheung, Y.-S.; Hsu, C.-W.; Ng, C. Y.; Huang, J.-C.; Li, W.-K.; Chiu, S.-W. *Int. J. Mass Spectrom. Ion Processes* **1996**, *159*, 13.
(27) Chiu, S.-W.; Li, W.-K.; Tzeng, W.-B.; Ng, C. Y. *J. Chem. Phys.* **1992**, *97*, 6557.
(28) The NIST Chemistry Webbook. http://webbook.nist.gov/chemistry/.